

Decoding Reed-Muller Codes with Successive Codeword Permutations

Nghia Doan, Seyyed Ali Hashemi, Marco Mondelli, and Warren J. Gross

Abstract

A novel recursive list decoding (RLD) algorithm of Reed-Muller (RM) codes based on successive permutations (SP) of the codeword is presented. An SP scheme that performs maximum likelihood decoding on a subset of the symmetry group of RM codes is first proposed to carefully select a good codeword permutation on the fly. Then, the proposed SP technique is applied to an improved RLD algorithm that initializes different decoding paths with random codeword permutations, which are sampled from the full symmetry group of RM codes. Finally, an efficient latency reduction scheme is introduced that virtually preserves the error-correction performance of the proposed decoder. Simulation results demonstrate that for the RM code of size 256 with 163 information bits, the proposed decoder reduces 39% of the computational complexity, 36% of the decoding latency, and 74% of the memory requirement of the state-of-the-art RLD algorithm with list size 64 that also uses the permutations from the full symmetry group of RM codes, while only incurring an error-correction performance degradation of 0.1 dB at the target frame error rate of 10^{-3} .

Index Terms

Reed-Muller codes, polar codes, 5G, codeword permutations.

I. INTRODUCTION

Reed-Muller (RM) codes are a class of error-correction codes discovered by Muller [1] and Reed [2], which were proven to achieve the capacity of erasure channels thanks to their large symmetry (automorphism) group [3]. RM codes are similar to polar codes under the factor-graph representation of the codes. The main difference between RM and polar codes is that RM codes are constructed to maximize the minimum distance among all the codewords [1], [2], while polar codes are constructed to minimize the error probability under successive-cancellation (SC) decoding [4]–[7] or SC list (SCL) decoding [8], [9]. An advantage of RM codes over polar codes is that the code construction of RM codes is channel-independent, which does not impose

additional complexity when the codes are constructed for different communication mediums, even under variable channel conditions.

It was shown in [10], [11] that with maximum likelihood (ML) decoding, RM codes achieve a better error-correction performance compared to polar codes. However, ML decoding is generally impractical due to its exponential complexity. As a consequence, RM codes are often decoded using sub-optimal decoders in practice, e.g., SC-based decoding [10], [12]–[14], SCL decoding [15]–[17], and recursive list decoding (RLD) [18]–[22]. Recently, a recursive projection-aggregation (RPA) decoding algorithm has been introduced to decode RM codes, whose error-correction performance is close to that of ML decoding [23]. However, RPA decoding in general is of higher complexity when compared with RLD decoding [24].

The error-correction performance of RM codes under various decoding algorithms can be significantly improved by utilizing their rich symmetry group [19], [20], [25]–[28]. Specifically, in [27], [28] a list of codeword permutations is selected and the decoding algorithm is performed on them. As RM and polar codes share the same factor-graph representation, it was observed in [29]–[33] that the error-correction performance of polar codes is also improved by running the decoding algorithms on a list of their factor-graph permutations. Since the decoders can be run in parallel on different permutations, the decoders proposed in [27]–[33] can provide a high decoding throughput at the cost of high memory consumption. In addition, it was discovered in [28] that utilizing the codeword permutations sampled from the full symmetry group of RM codes provides significant error-correction performance gain compared to the permutations sampled from the factor-graph permutation group of the codes. Instead of running each constituent decoder independently on a different permutation, the improved RLD algorithm introduced in [20] only performs permutation decoding until the first information bit is visited. Then, only the decoding operations in the information bit domain are carried out to select the L distinct best decoding paths, while keeping the permutations of all the active paths unchanged [20].

A successive permutation (SP) scheme was introduced in [26] to improve the error-correction performance of RM codes under SCL decoding. Specifically, during the course of SCL decoding, the SP technique recursively selects a cyclic factor-graph permutation of a RM code to maximize the reliability of the channel seen by its constituent codes [26]. It was shown that the error-correction performance of the SP-aided SCL (SP-SCL) decoder with a list size of L ($L \geq 2$) is similar to that of a conventional SCL decoder with a list size of $2L$ [26]. However, the permutation selection scheme in [26] assumes that all the constituent codes of a RM code are of

maximum order. Consequently, the SP-SCL decoder does not provide significant error-correction performance gains for low-order RM codes when a relatively small list size is used.

In this paper, we present a novel RLD-based algorithm of RM codes that provides better error-correction performance and complexity trade-offs in comparison with the state-of-the-art RM decoders introduced in [20], [28]. The contributions of this paper are as follows:

- 1) We generalize the SP scheme initially proposed in [20] as a decoding problem and perform ML decoding on a subset of the full symmetry group of RM codes to carefully select a good codeword permutation on the fly.
- 2) We propose an improved RLD algorithm that utilizes the generalized SP scheme. In particular, at the beginning of the decoding process, the proposed decoder initializes L decoding paths with L random codeword permutations sampled from the full symmetry group of RM codes. Then, the proposed SP scheme is independently applied to each active decoding path for all the constituent RM codes visited. Furthermore, an effective latency reduction scheme is incorporated in the proposed algorithm that relatively preserves its error-correction performance.

Note that the proposed RLD algorithm utilizes existing fast and efficient decoding techniques to perform ML decoding for the first-order and single parity-check (SPC) constituent RM codes as introduced in [18] and [22], respectively. Our simulation results demonstrate that for the RM code of size 256 with 163 information bits, the proposed decoder reduces 39% of the computational complexity, 36% of the decoding latency, and 74% of the memory requirement of the state-of-the-art RLD algorithm with list size 64 that also uses the permutations from the full symmetry group of RM codes [20], [28], while only incurring an error-correction performance degradation of 0.1 dB at the target frame error rate (FER) of 10^{-3} . For the same RM code and also at the target FER of 10^{-3} , the proposed decoder reduces 27% of the computational complexity and provides a memory reduction of $14.4\times$ compared to the permuted simplified SC decoder with 128 random permutations [28], at the costs of $5.5\times$ increase in the decoding latency and a negligible FER performance degradation.

The remainder of this paper is organized as follows. Section II introduces the backgrounds on RM codes and their factor graph-based decoding algorithms. Section III provides details of the proposed decoding techniques and their performance evaluation considering the error-correction performance, computational complexity, decoding latency, and memory requirement. Finally, concluding remarks are drawn in Section IV.

II. PRELIMINARIES

Throughout this paper, boldface letters indicate vectors and matrices. Unless otherwise specified, non-boldface letters indicate either binary, integer or real numbers. Greek letters are used to denote a RM code (node), the log-likelihood ratio (LLR) values, and the hard decisions associated with a RM code. Finally, sets are denoted by blackboard bold letters, e.g., \mathbb{R} is the set containing real numbers.

A. Reed-Muller Codes

A RM code is specified by a pair of integers $0 \leq r \leq m$ and is denoted as $\mathcal{RM}(r, m)$, where r is the order of the code. $\mathcal{RM}(r, m)$ has a code length $N = 2^m$ with $K = \sum_{i=0}^r \binom{m}{i}$ information bits, and a minimum distance $d = 2^{m-r}$. A RM code is constructed by applying a linear transformation to the binary message word $\mathbf{u} = \{u_0, u_1, \dots, u_{N-1}\}$ as $\mathbf{x} = \mathbf{u}\mathbf{G}^{\otimes m}$ where $\mathbf{x} = \{x_0, x_1, \dots, x_{N-1}\}$ is the codeword and $\mathbf{G}^{\otimes m}$ is the m -th Kronecker power of the matrix $\mathbf{G} = \begin{bmatrix} 1 & 0 \\ 1 & 1 \end{bmatrix}$ [34]. The element u_i of \mathbf{u} is fixed to 0 if the weight of the i -th row of $\mathbf{G}^{\otimes m}$, denoted as w_i , is smaller than d . Formally, $u_i = 0 \forall i \in \mathbb{F}$, where $\mathbb{F} = \{i | 0 \leq i < N, w_i < d\}$. In addition, we denote by \mathbb{I} the set of information bits, i.e., $\mathbb{I} = \{i | 0 \leq i < N, w_i \geq d\}$, and \mathbb{I} and \mathbb{F} are known to both the encoder and the decoder.

In this paper, the codeword \mathbf{x} is modulated using binary phase-shift keying (BPSK) modulation, and an additive white Gaussian noise (AWGN) channel model is considered. Therefore, the soft vector of the transmitted codeword received by the decoder is given as $\mathbf{y} = (\mathbf{1} - 2\mathbf{x}) + \mathbf{z}$, where $\mathbf{1}$ is an all-one vector of size N , and $\mathbf{z} \in \mathbb{R}^N$ is a Gaussian noise vector with variance σ^2 and zero mean. In the log-likelihood ratio (LLR) domain, the LLR vector of the transmitted codeword is given as $\boldsymbol{\alpha}_m = \ln \frac{Pr(\mathbf{x}=0|\mathbf{y})}{Pr(\mathbf{x}=1|\mathbf{y})} = \frac{2\mathbf{y}}{\sigma^2}$. Fig. 1a illustrates the encoding process of $\mathcal{RM}(1, 3)$ using the factor-graph representation of the code, where $N = 8$, $K = 4$, and $\mathbb{I} = \{3, 5, 6, 7\}$. It was shown in [35, Chapter 14] that for RM codes of order $r = 1$, the ML decoding algorithm can be efficiently implemented by utilizing a fast Hadarmard transform (FHT). In the next sections, we summarize various decoding algorithms used to decode RM codes of order $r > 1$.

B. Successive-Cancellation and Successive-Cancellation List Decoding

SC decoding is executed on the factor-graph representation of the code [10]. To obtain the message word, the soft LLR values and the hard bit estimations are propagated through all the

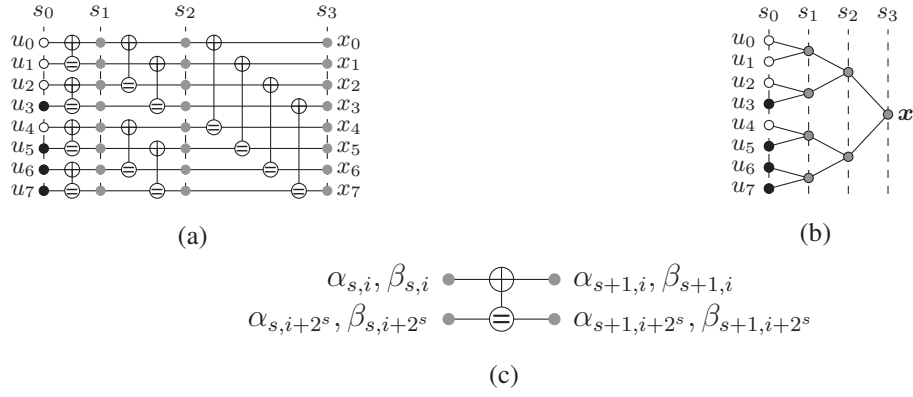


Fig. 1: (a) Factor-graph representation of $\mathcal{RM}(1, 3)$, (b) binary tree representation of $\mathcal{RM}(1, 3)$, and (c) a PE.

processing elements (PEs), which are depicted in Fig. 1c. Each PE performs the following computations: $\alpha_{s,i} = f(\alpha_{s+1,i}, \alpha_{s+1,i+2^s})$ and $\alpha_{s,i+2^s} = g(\alpha_{s+1,i}, \alpha_{s+1,i+2^s}, \beta_{s,i})$, where $\alpha_{s,i}$ and $\beta_{s,i}$ are the soft LLR value and the hard-bit estimation at the s -th stage and the i -th bit, respectively. The min-sum approximation formulations of f and g are $f(a, b) = \min(|a|, |b|) \text{sgn}(a) \text{sgn}(b)$, and $g(a, b, c) = b + (1 - 2c)a$, where $a, b \in \mathbb{R}$ and $c \in \{0, 1\}$. The soft LLR values at the m -th stage are initialized to α_m and the hard-bit estimation of an information bit at the 0-th stage is obtained as $\hat{u}_i = \beta_{0,i} = \frac{1 - \text{sgn}(\alpha_{0,i})}{2}$, $\forall i \in \mathbb{I}$. The hard-bit values of the PE are then computed as $\beta_{s+1,i} = \beta_{s,i} \oplus \beta_{s,i+2^s}$ and $\beta_{s+1,i+2^s} = \beta_{s,i+2^s}$.

SCL decoding was introduced in [15]–[17] to improve SC decoding of polar and RM codes by maintaining a list of L best SC decoding paths. Under SCL decoding, the estimation of a message bit \hat{u}_i ($i \in \mathbb{I}$) is considered to be both 0 and 1, i.e., a path split. Thus, the number of candidate codewords (decoding paths) doubles after each information bit is estimated. To prevent the exponential growth of the number of decoding paths, a path metric is utilized to select the L most probable decoding paths after each information bit is decoded. In the LLR domain, the low-complexity path metric can be obtained as [17]

$$\text{PM}_l = \begin{cases} \text{PM}_l + |\alpha_{0,i_l}| & \text{if } \hat{u}_i \neq \frac{1 - \text{sgn}(\alpha_{0,i_l})}{2}, \\ \text{PM}_l & \text{otherwise,} \end{cases} \quad (1)$$

where α_{0,i_l} denotes the soft value of the i -th bit at stage 0 of the l -th path, and initially $\text{PM}_l = 0$ $\forall l$. At the end of the decoding process, only the path that has the smallest path metric is selected as the decoding output.

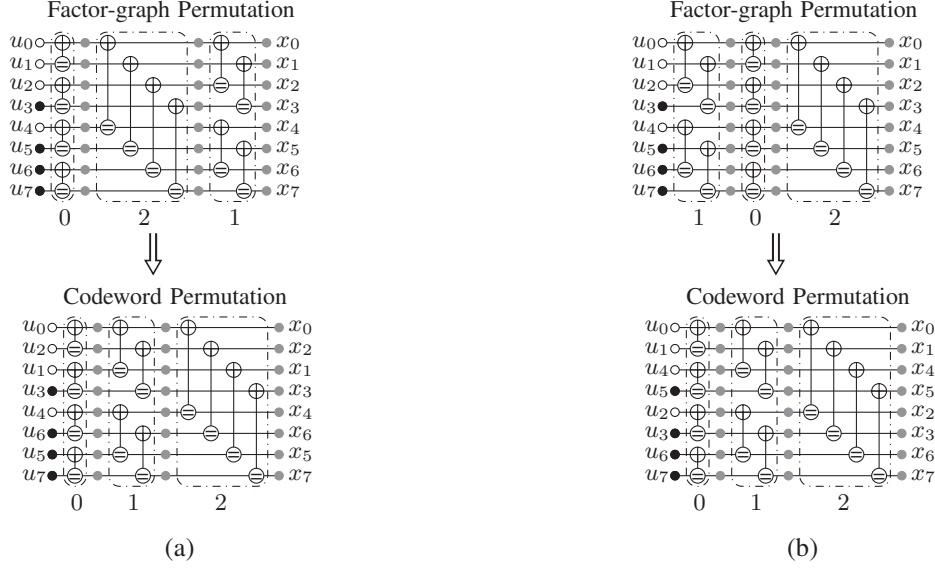


Fig. 2: The equivalent codeword permutations of the factor-graph permutations (a) $\{0, 2, 1\}$ and (b) $\{1, 0, 2\}$, under the original factor-graph representation with the PE layers indexed as $\{0, 1, 2\}$.

C. Successive Permutations for SCL Decoding

SC and SCL decoding can also be illustrated on a binary tree representation of the code [12], [36]. Fig. 1b shows a full binary tree representation of $\mathcal{RM}(1, 3)$, whose factor graph is depicted in Fig. 1a. Consider a parent node ν located at the s -th stage ($s > 0$) of the binary tree, which is a RM code specified by a pair of parameters (r_ν, m_ν) with $m_\nu = s$. There are N_ν LLR values and N_ν hard decisions associated with this node, where $N_\nu = 2^{m_\nu}$. Let $\alpha_l^{(\nu)}$ and $\beta_l^{(\nu)}$ be the soft and hard values associated with the parent node ν of the l -th decoding path, respectively. $\alpha_l^{(\nu)}$ and $\beta_l^{(\nu)}$ are defined as

$$\begin{cases} \alpha_l^{(\nu)} = \{\alpha_{s, i_{\min \nu_l}}^{(\nu)}, \dots, \alpha_{s, i_{\max \nu_l}}^{(\nu)}\}, \\ \beta_l^{(\nu)} = \{\beta_{s, i_{\min \nu_l}}^{(\nu)}, \dots, \beta_{s, i_{\max \nu_l}}^{(\nu)}\}, \end{cases}$$

where $i_{\min \nu_l}$ and $i_{\max \nu_l}$ are the bit indices such that $0 \leq i_{\min \nu_l} < i_{\max \nu_l} \leq N - 1$ and $i_{\max \nu_l} - i_{\min \nu_l} = N_\nu - 1$. The hard-decision values of ν in the bipolar form are denoted as $\eta_l^{(\nu)} = \{\eta_{s, i_{\min \nu_l}}^{(\nu)}, \dots, \eta_{s, i_{\max \nu_l}}^{(\nu)}\}$, where $\eta_{s, i}^{(\nu)} = 1 - 2\beta_{s, i}^{(\nu)}$, $i_{\min \nu_l} \leq i \leq i_{\max \nu_l}$.

A factor-graph permutation is constructed by permuting the PE stages of the RM code's factor graph [11]. Fig. 2 illustrates examples of the factor-graph permutations of $\mathcal{RM}(1, 3)$ whose original factor-graph representation is presented in Fig. 1a, where the PE layers of the original

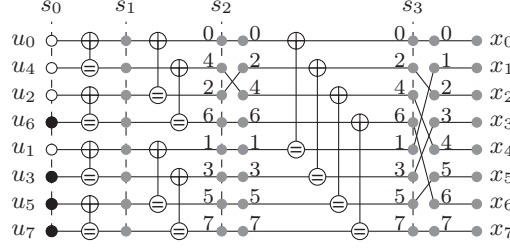


Fig. 3: An example of the SP technique introduced in [26] when applied to $\mathcal{RM}(1,3)$.

factor graph in Fig. 1a are indexed as $\{0, 1, 2\}$. Fig. 2 also illustrates the conversion from the factor-graph permutations to the codeword permutations used in [20], which is defined as follows. Let $\mathbf{b}_i = \{b_{m-1_i}, \dots, b_{0_i}\}$ be a binary expansion of the bit index i , and $\pi : \{0, \dots, m-1\} \rightarrow \{0, \dots, m-1\}$ be a permutation of the PE layers of $\mathcal{RM}(r, m)$. The permuted bit index of i given π in the binary expansion is $\mathbf{b}_{\pi(i)} = \{b_{\pi(m-1)_i}, \dots, b_{\pi(0)_i}\}$, where $0 \leq i < 2^m$ [20].

The SP technique carefully selects a single codeword permutation on the fly to significantly improve the error probability of SCL decoding. Given a permutation $\pi \in \mathcal{P}_s$, the $f(\cdot)$ functions when applied to the permuted LLR values associated with the parent node ν generate an LLR vector corresponding to its left-child node λ , denoted as $\boldsymbol{\alpha}^{(\lambda)} = \{\alpha_{s-1, i_{\min_\lambda}}^{(\lambda)}, \dots, \alpha_{s-1, i_{\max_\lambda}}^{(\lambda)}\}^1$. The factor-graph permutation π^* of ν is selected to maximize the channel reliabilities corresponding to λ , which allows for a better estimation of λ under SC and SCL decoding [26]. The selection criteria of π^* is given as [26]

$$\pi^* = \arg \max_{\pi \in \mathcal{P}_s} \sum_{i=i_{\min_\lambda}}^{i_{\max_\lambda}} |\alpha_{s-1, i}^{(\lambda)}|. \quad (2)$$

The SP technique considers cyclic factor-graph permutations to be included in the set \mathcal{P}_s [26]. For instance, the cyclic permutations of $\mathcal{RM}(1,3)$ are $\{0, 1, 2\}$, $\{2, 0, 1\}$, and $\{1, 2, 0\}$. Fig. 3 shows an example of the SP technique applied to $\mathcal{RM}(1,3)$, where the permuted factor graphs are transformed to the permuted bit indices as in [20]. In Fig. 3, let π^* be the factor-graph permutation applied to the bit indices $I = \{0, 2, 4, 6\}$ at stage s_2 , corresponding to $\mathcal{RM}(0,2)$. The equivalent codeword permutation of π^* is $\{0, 1, 2, 3\} \rightarrow \{0, 2, 1, 3\}$. Thus, $I = \{0, 2, 4, 6\} \xrightarrow{\pi^*} I_{\pi^*} = \{0, 4, 2, 6\}$, where I_{π^*} is the resulting permuted bit indices of I . On the other hand, the best

¹In the rest of the paper, as the permutation selection scheme is applied independently for each decoding path, we drop the subscript l for clarity.

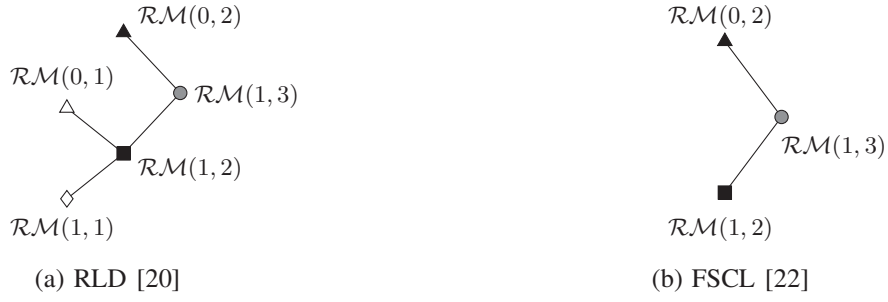


Fig. 4: Binary tree representations of $\mathcal{RM}(1, 3)$ under (a) RLD [20] and (b) FSCL [22].

factor-graph permutation selected for the $\mathcal{RM}(1, 2)$ code at stage s_2 is the original permutation.

D. Recursive List Decoding with Permutations

The RLD algorithms introduced in [18], [20] utilize ML decoding to decode the special constituent RM codes at the parent node level, instead of fully traversing the binary tree as in SCL decoding. Similarly, in [21], [22], the authors proposed fast SCL (FSCL) decoding algorithms for various special constituent polar codes, which are also RM codes. The RLD and FSCL decoding algorithms preserve the error-correction performance of SCL decoding and completely remove the need to traverse the binary tree when special nodes are encountered. Therefore, the latency of RLD and FSCL decoding is significantly smaller than SCL decoding. In particular, $\mathcal{RM}(0, m_\nu)$ (repetition (Rep) code) and $\mathcal{RM}(m_\nu - 1, m_\nu)$ (SPC code) are considered under FSCL decoding [22]. The RLD algorithm based on FHT (FHT-RLD) in [18] and the RLD algorithm in [20] perform fast decoding for $\mathcal{RM}(0, m_\nu)$ (first-order RM code) and $\mathcal{RM}(m_\nu, m_\nu)$ (Rate-1 code). Fig. 4 shows an example of the binary tree representations used by RLD [20] and FSCL [22] for decoding $\mathcal{RM}(1, 3)$, while under FHT-RLD [18], $\mathcal{RM}(1, 3)$ is directly decoded using FHT without decomposing the code to smaller RM codes.

An improvement scheme that runs the RLD algorithm on random factor-graph permutations was proposed in [20] and is referred to as the RLDP algorithm in this paper. The RLDP algorithm on $\mathcal{RM}(r, m)$ initially runs $\binom{m}{r}$ independent decoding paths with each path performing SC decoding on a different factor-graph permutation [20]. After each information bit is decoded, RLDP performs the path extension/pruning operations in the information bit domain to maintain the list of L best decoding paths, while keeping the predetermined codeword permutations of the active decoding paths unchanged [20]. In this paper, we directly run the RLD algorithm in [20] on the full symmetry group of the codes and we refer to this decoding algorithm as RLDA.

III. SUCCESSIVE PERMUTATIONS FOR RECURSIVE LIST DECODING OF REED-MULLER CODES

In this section, a generalized SP scheme for the RLD-based algorithms of RM codes is first proposed. We then provide details on the integration of the proposed SP scheme into an improved RLD-based algorithm. Finally, we numerically analyze the error-correction performance, computational complexity, decoding latency, and memory requirement of the proposed decoder and compare them with those of the state-of-the-art RM decoders.

A. Improved Successive Permutation Scheme

The selection criteria in (2), which is used in [26], is an oversimplification that does not take into account the existing parity constraints in the code. In fact, it treats all the constituent RM codes λ as Rate-1 codes. This oversimplification becomes inaccurate, especially for low-order RM codes, as the number of information bits is significantly smaller than $N_\lambda = 2^{s-1}$. Consequently, the error probability of the SP scheme in [26] for SCL decoding on low-order RM codes is not satisfactory, especially when a small to moderate list size is used.

To tackle this issue, we propose an accurate SP scheme that selects the best factor-graph permutation π^* by performing ML decoding on the symmetry group of RM codes. The proposed selection criteria is given as

$$\pi^* = \arg \max_{\pi \in \mathcal{P}_s} M_\pi(\boldsymbol{\alpha}^{(\lambda)}), \quad (3)$$

where $M_\pi(\boldsymbol{\alpha}^{(\lambda)})$ is the factor-graph permutation metric of π when π is applied to the parent node ν that is calculated as

$$M_\pi(\boldsymbol{\alpha}^{(\lambda)}) = \max_{\forall \boldsymbol{\eta}^{(\lambda)}} \sum_{i=i_{\min_\lambda}}^{i_{\max_\lambda}} \eta_{s-1,i}^{(\lambda)} \alpha_{s-1,i}^{(\lambda)}, \quad (4)$$

with $\boldsymbol{\eta}_\lambda$ being the hard decisions of a valid codeword corresponding to λ . It can be observed that if λ is a Rate-1 code, (3) reverts to (2) as $\eta_{s-1,i}^{(\lambda)}$ is set to $\text{sgn}(\alpha_{s-1,i}^{(\lambda)})$ to maximize the likelihood of $\boldsymbol{\eta}_\lambda$ and $\boldsymbol{\alpha}_\lambda$. The elements of $\boldsymbol{\eta}_\lambda$ can be calculated by performing ML decoding on λ . However, ML decoding is generally of high complexity. Therefore, in this paper we derive $M_\pi(\boldsymbol{\alpha}^{(\lambda)})$ for special cases of λ for which the ML decoding operations can be realized with low complexity. Unlike [26], the set \mathcal{P}_s considered in this paper contains the general codeword permutations sampled from the full symmetry group of the codes [28]. Nevertheless, we limit

the maximum number of permutations stored in \mathcal{P}_s to s , which is equal to the number of cyclic factor-graph permutations as considered in [26].

Since first-order constituent RM codes can be decoded efficiently using ML decoding [35, Chapter 14], the permutation metric $M_\pi(\alpha^{(\lambda)})$ can be efficiently calculated if λ is a first-order RM code. When λ is of order 2 or higher, we propose to simplify the computation of $M_\pi(\alpha^{(\lambda)})$ by using (2). The calculation of $M_\pi(\alpha^{(\lambda)})$ for the considered special nodes in this paper is summarized as follows.

1) $\mathcal{RM}(1, s-1)$: The metric $M_\pi(\alpha^{(\lambda)})$ is the likelihood of the best decoding path of λ given $\alpha^{(\lambda)}$, which can be calculated efficiently using FHT decoding [35, Chapter 14].

2) $\mathcal{RM}(r_\lambda, s-1)$ ($r_\lambda \geq 2$): We use (2) to calculate $M_\pi(\alpha^{(\lambda)})$ for constituent RM codes of order $r_\lambda \geq 2$ as

$$M_\pi(\alpha^{(\lambda)}) = \sum_{i=i_{\min_\lambda}}^{i_{\max_\lambda}} |\alpha_{s-1,i}|. \quad (5)$$

B. Improved Recursive List Decoding with Successive Permutation

We now propose an improved RLD algorithm that utilizes the SP scheme introduced in Section III-A. The details of the proposed algorithm are provided in Algorithm 1². In the beginning of Algorithm 1, the proposed algorithm with list size L initializes all the L decoding paths with L random codeword permutations sampled from the symmetry group of RM codes. Each decoding path with index l ($0 \leq l < L$) associated with $\mathcal{RM}(r, m)$ is characterized by a data structure $\mathcal{Q}_{(r,m)}$ that stores the channel LLR vector α , the path metric PM, the estimated codeword \hat{x} , and the initial codeword permutation π_{init} . The recursive decoding algorithm utilizing the SP scheme, denoted as the $\text{SP-RLD}(\cdot)$ function, is then applied to the initialized data structures $\{\mathcal{Q}_{(r,m)}[0], \dots, \mathcal{Q}_{(r,m)}[L-1]\}$, and returns the updated data structures of the L best decoding paths. Next, the updated path metrics of all the estimated decoding paths given by the $\text{SP-RLD}(\cdot)$ function are sorted, where the output of the sorting function is the best decoding path with index l^* that has the smallest path metric. The initial codeword permutation π_{init}^* associated with the best decoding path l^* is then obtained. Finally, an inverted permutation $(\pi_{\text{init}}^*)^{-1}$ is applied to the best candidate codeword $\mathcal{Q}_{(r,m)}[l^*].\hat{x}$ to obtain the final estimated codeword \hat{x} .

In Algorithm 2, we provide the details of the $\text{SP-RLD}(\cdot)$ function. If the constituent RM codes are of order 1 or $m-1$, the ML decoders of the first-order RM codes ($\text{FHT-List}(\cdot)$)

²The C++ implementation of the proposed decoder is provided in <https://github.com/nghiadt05/SPRLD>.

Algorithm 1: Improved RLD with SP of RM Codes

```

Input :  $\mathbf{y}$ 
Output:  $\hat{\mathbf{x}}$ 
  /* Initialize  $L$  random codeword permutations associated with  $L$  decoding paths */
1 for  $l \leftarrow 0$  to  $L - 1$  do
2    $\pi_l : \mathbf{y} \xrightarrow{\pi_l} \mathbf{y}_{\pi_l}$ 
3    $\mathcal{Q}_{(r,m)}[l].\pi_{\text{init}} \leftarrow \pi_l; \mathcal{Q}_{(r,m)}[l].\boldsymbol{\alpha} \leftarrow \mathbf{y}_{\pi_l}$ 
4    $\mathcal{Q}_{(r,m)}[l].\text{PM} \leftarrow 0; \mathcal{Q}_{(r,m)}[l].\hat{\mathbf{x}} \leftarrow \mathbf{0}$ 

  /* Improved RLD with SP */
5  $\mathcal{Q}_{(r,m)}[0], \dots, \mathcal{Q}_{(r,m)}[L - 1] \leftarrow \text{SP-RLD}(\mathcal{Q}_{(r,m)}[0], \dots, \mathcal{Q}_{(r,m)}[L - 1])$ 

  /* Selection of the best decoding path */
6  $l^* \leftarrow \text{Sort}(\mathcal{Q}_{(r,m)}[0].\text{PM}, \dots, \mathcal{Q}_{(r,m)}[L - 1].\text{PM})$ 
7  $\pi_{\text{init}}^* \leftarrow \mathcal{Q}_{(r,m)}[l^*].\pi_{\text{init}}$ 
8  $(\pi_{\text{init}}^*)^{-1} : \mathcal{Q}_{(r,m)}[l^*].\hat{\mathbf{x}} \xrightarrow{(\pi_{\text{init}}^*)^{-1}} \hat{\mathbf{x}}$ 
9 return  $\hat{\mathbf{x}}$ 

```

[18]) or that of the SPC codes (SPC-List(\cdot) [22]) is queried to obtain the estimated codewords of the best L decoding paths and their path metrics, respectively. Note that as the FHT-List(\cdot) [18] and SPC-List(\cdot) functions perform ML decoding at the parent node level, no codeword permutation is required to obtain the optimal decoding outputs of the L best decoding paths. On the other hand, if the constituent code $\mathcal{RM}(r, m)$ satisfies $1 < r < m - 1$, the SP-RLD(\cdot) function is recursively queried to decode the left and right child nodes $\mathcal{RM}(r - 1, m - 1)$ and $\mathcal{RM}(r, m - 1)$ of $\mathcal{RM}(r, m)$, respectively, whose decoding results are used to construct the decoding output of $\mathcal{RM}(r, m)$. Specifically, from line 6 to line 20 of Algorithm 2, the best permutations of $\mathcal{RM}(r, m)$ are obtained independently for each decoding path with index l , using the proposed SP scheme. By π_{tmp} we indicate a random permutation of $\mathcal{RM}(r, m)$, which is used to obtain the LLR values associated with the right child $\mathcal{RM}(r - 1, m - 1)$, i.e., $\boldsymbol{\alpha}^{(\lambda)}$, followed by the permutation metric computation specified in Section III-A. If a better permutation π_{tmp} is found for the l -th decoding path, the selected permutation π_{SP} is updated in the data structure $\mathcal{Q}_{(r,m)}[l]$, which is required to perform the inverted permutation after the right-child node $\mathcal{RM}(r, m - 1)$ is decoded. In addition, the data structures of the left-child nodes $\mathcal{Q}_{(r-1,m-1)}$ are also initialized during the permutation selection of $\mathcal{RM}(r, m)$. Given the initialized data structures of the left-child node $\mathcal{Q}_{(r-1,m-1)}$, the SP-RLD(\cdot) function is then queried to obtain the updated data structures $\mathcal{Q}_{(r-1,m-1)}$ corresponding to the L best decoding

Algorithm 2: SP-RLD(\cdot)

```

Input :  $\mathcal{Q}_{(r,m)}[0], \dots, \mathcal{Q}_{(r,m)}[L-1]$ 
Output:  $\mathcal{Q}_{(r,m)}[0], \dots, \mathcal{Q}_{(r,m)}[L-1]$ 
1 if  $r = 1$  then
2    $\mathcal{Q}_{(r,m)}[0], \dots, \mathcal{Q}_{(r,m)}[L-1] \leftarrow \text{FHT-List}(\mathcal{Q}_{(r,m)}[0], \dots, \mathcal{Q}_{(r,m)}[L-1])$ 
3 else if  $r = m-1$  then
4    $\mathcal{Q}_{(r,m)}[0], \dots, \mathcal{Q}_{(r,m)}[L-1] \leftarrow \text{SPC-List}(\mathcal{Q}_{(r,m)}[0], \dots, \mathcal{Q}_{(r,m)}[L-1])$ 
5 else
6   /* Decode the left-child node with SP */
7   for  $l \leftarrow 0$  to  $L-1$  do
8      $\mathcal{Q}_{(r-1,m-1)}[l].\pi_{\text{init}} \leftarrow \mathcal{Q}_{(r,m)}[l].\pi_{\text{init}}$ 
9      $\mathcal{Q}_{(r-1,m-1)}[l].\text{PM} \leftarrow \mathcal{Q}_{(r,m)}[l].\text{PM}$ 
10     $M^* \leftarrow -\infty$ 
11    for  $p \leftarrow 0$  to  $m-1$  do
12       $\pi_{\text{tmp}} : \mathcal{Q}_{(r,m)}[l].\alpha \xrightarrow{\pi_{\text{tmp}}} \alpha_{\text{tmp}}$ 
13       $\alpha^{(\lambda)} \leftarrow f(\alpha_{\text{tmp}})$ 
14      if  $r = 2$  then
15        Compute  $M_{\pi_{\text{tmp}}}(\alpha^{(\lambda)})$  using FHT
16      else if  $r > 2$  then
17        Compute  $M_{\pi_{\text{tmp}}}(\alpha^{(\lambda)})$  using (5)
18      if  $M_{\pi_{\text{tmp}}}(\alpha^{(\lambda)}) > M^*$  then
19         $\mathcal{Q}_{(r-1,m-1)}[l].\alpha \leftarrow \alpha^{(\lambda)}$ 
20         $\mathcal{Q}_{(r,m)}[l].\pi_{\text{SP}} \leftarrow \pi_{\text{tmp}}$ 
21         $M^* \leftarrow M_{\pi_{\text{tmp}}}(\alpha^{(\lambda)})$ 
22   $\mathcal{Q}_{(r-1,m-1)}[0], \dots, \mathcal{Q}_{(r-1,m-1)}[L-1] \leftarrow$ 
23    SP-RLD( $\mathcal{Q}_{(r-1,m-1)}[0], \dots, \mathcal{Q}_{(r-1,m-1)}[L-1]$ )
24  /* Decode the right-child node */
25  for  $l \leftarrow 0$  to  $L-1$  do
26     $\mathcal{Q}_{(r,m-1)}[l].\pi_{\text{init}} \leftarrow \mathcal{Q}_{(r-1,m-1)}[l].\pi_{\text{init}}$ 
27     $\mathcal{Q}_{(r,m-1)}[l].\text{PM} \leftarrow \mathcal{Q}_{(r-1,m-1)}[l].\text{PM}$ 
28     $\mathcal{Q}_{(r,m-1)}[l].\alpha \leftarrow g(\mathcal{Q}_{(r-1,m-1)}[l].\hat{x}, \mathcal{Q}_{(r,m)}[l_{\text{org}}^{(r,m)}].\alpha)$ 
29   $\mathcal{Q}_{(r,m-1)}[0], \dots, \mathcal{Q}_{(r,m-1)}[L-1] \leftarrow \text{SP-RLD}(\mathcal{Q}_{(r,m-1)}[0], \dots, \mathcal{Q}_{(r,m-1)}[L-1])$ 
30  /* Repermute the decoded codewords */
31  for  $l \leftarrow 0$  to  $L-1$  do
32     $\mathcal{Q}_{(r,m)}^{\text{tmp}}[l].\pi_{\text{init}} \leftarrow \mathcal{Q}_{(r,m-1)}[l].\pi_{\text{init}}$ 
33     $\mathcal{Q}_{(r,m)}^{\text{tmp}}[l].\text{PM} \leftarrow \mathcal{Q}_{(r,m-1)}[l].\text{PM}$ 
34     $\mathcal{Q}_{(r,m)}^{\text{tmp}}[l].\hat{x} \leftarrow \text{Concat}(\mathcal{Q}_{(r-1,m-1)}[l_{\text{org}}^{(r-1,m-1)}].\hat{x},$ 
35       $\mathcal{Q}_{(r-1,m-1)}[l_{\text{org}}^{(r-1,m-1)}].\hat{x} \oplus \mathcal{Q}_{(r,m-1)}[l].\hat{x})$ 
36     $\pi_{\text{SP}} \leftarrow \mathcal{Q}_{(r,m)}[l_{\text{org}}^{(r,m)}].\pi_{\text{SP}}$ 
37     $(\pi_{\text{SP}})^{-1} : \mathcal{Q}_{(r,m)}^{\text{tmp}}[l].\hat{x} \xrightarrow{(\pi_{\text{SP}})^{-1}} \mathcal{Q}_{(r,m)}^{\text{tmp}}[l].\hat{x}$ 
38  for  $l \leftarrow 0$  to  $L-1$  do
39     $\mathcal{Q}_{(r,m)}[l] \leftarrow \mathcal{Q}_{(r,m)}^{\text{tmp}}[l]$ 
40 return  $\mathcal{Q}_{(r,m)}[0], \dots, \mathcal{Q}_{(r,m)}[L-1]$ 

```

paths of the left-child node.

The decoding of the right-child nodes $\mathcal{RM}(r, m-1)$ is specified in line 22 to line 26 of Algorithm 2. The $g(\cdot)$ functions are used to obtain the LLR values of the right-child nodes, given the hard estimations of the left-child node, i.e., $\mathcal{Q}_{(r-1, m-1)}[l].\hat{\mathbf{x}}$, and the corresponding LLR values of the parent node where the left-child node is originated from, i.e., $\mathcal{Q}_{(r, m)}[l_{\text{org}}^{(r, m)}].\alpha$. Here, by $l_{\text{org}}^{(r, m)}$ we indicate the path index of the parent node from which the surviving left-child node is derived. After the decoding of the right-child nodes is finished, the estimated codewords of the L best paths associated with the parent node $\mathcal{RM}(r, m)$ are obtained based on the estimated hard values of the left-child and the right-child nodes (see lines 30 and 31), where $\text{Concat}(\mathbf{a}, \mathbf{b})$ indicates the concatenation of the binary vectors \mathbf{a} and \mathbf{b} . In addition, $\mathcal{Q}_{(r-1, m-1)}[l_{\text{org}}^{(r-1, m-1)}].\hat{\mathbf{x}}$ indicates the hard values of the left-child that corresponds to the l -th active decoding path $\mathcal{Q}_{(r, m-1)}[l].\hat{\mathbf{x}}$ of the right-child node. Next, $\mathcal{Q}_{(r, m)}[l_{\text{org}}^{(r, m)}].\pi_{\text{SP}}$, the codeword permutation previously selected for the parent node from which the l -th active decoding path of the right-child node is originated from, is used to re-permute the estimated codeword of the parent node. Finally, the data structures $\{\mathcal{Q}_{(r, m)}[0], \dots, \mathcal{Q}_{(r, m)}[L-1]\}$ of the L best decoding paths for the parent node $\mathcal{RM}(r, m)$ are returned as the outputs of the recursive $\text{SP-RLD}(\cdot)$ function. Note that we keep track of the initial permutation π_{init} applied to the parent code for each active decoding path during the course of decoding.

As the constituent RM codes are decoded successively under the proposed decoder, we further propose a complexity and decoding latency reduction scheme that only applies the SP operations for the first S ($S \geq 0$) left-child nodes. Fig. 5 illustrates an example of the proposed decoding algorithm when applied to $\mathcal{RM}(3, 5)$ using $S \in \{2, 1\}$. In Fig. 5(a), since the left-child node of $\mathcal{RM}(3, 5)$ is a RM code of order 2, the codeword permutation of $\mathcal{RM}(3, 5)$ is selected using the selection criteria in (5). Then, the LLR values associated with $\mathcal{RM}(2, 4)$ are obtained with the f functions. Since the left-child node of $\mathcal{RM}(2, 4)$ is a first-order RM code, FHT decoding [18] is used to select the best permutation for $\mathcal{RM}(2, 4)$, followed by the FHT-List decoder applied on the list of L decoding paths with the selected codeword permutations for $\mathcal{RM}(2, 4)$. Finally, as all the right-child RM codes are SPC codes, SPC-List decoding is used to decode them. The similar decoding operations are carried out for $\mathcal{RM}(2, 5)$ in Fig. 5(b) except that the SP operations are only applied to the parent node of the first left-child node, while the original permutations are used for the parent node $\mathcal{RM}(2, 4)$ of the second left-child node.

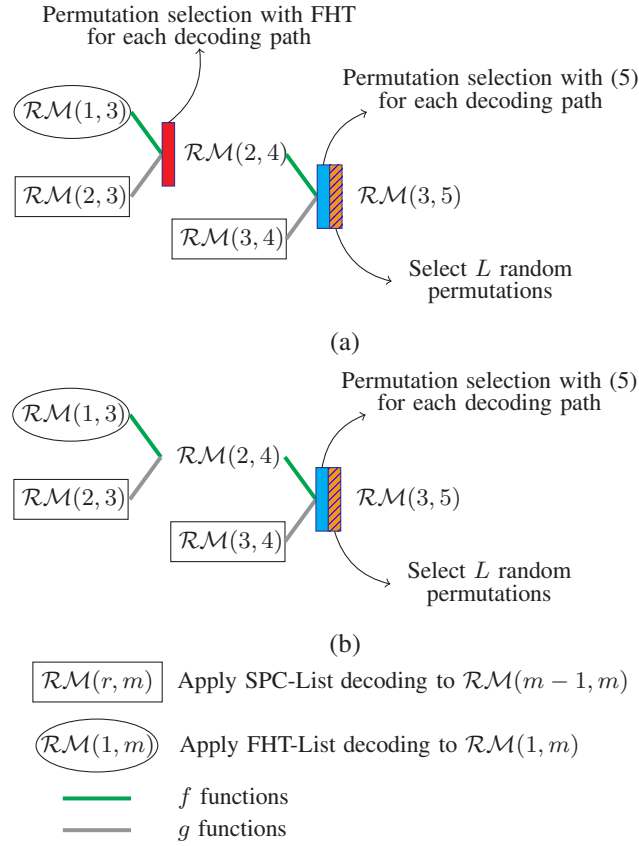


Fig. 5: Examples of the proposed decoder when applied to $\mathcal{RM}(3, 5)$ with (a) $S = 2$ and (b) $S = 1$.

C. Performance Evaluation

1) *Quantitative Complexity Analysis:* In this paper, we consider sequential and parallel implementations of the permutation selection scheme in (3). Under the sequential implementation of (3), a similar memory consumption as SC-based decoders is required to store the internal LLR values [26]. On the other hand, under the parallel implementation, a memory of $mLNQ$ bits is required to store the internal LLR values, where m is the maximum number of the candidate permutations for the SP scheme, and Q is the number of quantization bits. In addition, the SP scheme in both the sequential and parallel implementations requires mQ memory bits to store the permutation metric $M_\pi(\alpha^{(\lambda)})$. Throughout this paper, we use $Q = 32$ for all the considered decoders. Note that the FHT operations compute and store the new LLR values directly to $\alpha^{(\lambda)}$, thus no extra memory is needed under FHT decoding. Table I summarizes the memory requirements of the proposed decoders in this paper denoted as SP-RLD- L ($L \geq 1$) and SSP-

TABLE I: Memory requirements in terms of the number of bits required by the proposed decoders.

Decoding Algorithm		Memory Requirement
SP-RLD-1 SSP-RLD- S -1	(sequential)	$2NQ + mQ + N$
SP-RLD-1 SSP-RLD- S -1	(parallel)	$(m + 1)NQ + mQ + N$
SP-RLD- L SSP-RLD- S - L	($L > 1$, sequential)	$N(L + 1)Q + mQ + 2NL$
SP-RLD- L SSP-RLD- S - L	($L > 1$, parallel)	$N(mL + 1)Q + mQ + 2NL$

RLD- S - L , where SSP-RLD- S - L is the simplified version of SP-RLD- L in which the SP scheme is only applied to the first S ($S > 0$) left-child nodes.

The decoding latency of the proposed decoders is computed by counting the number of time steps required by all the decoding operations. We assume that there is no resource constraint. Thus, all concurrent operations in $f(\cdot)$ and $g(\cdot)$ functions, the path metric computations, and the computations of $M_\pi(\alpha^{(\lambda)})$ in (5) require one time step [21], [22]. The permutation metric $M_\pi(\alpha^{(\lambda)})$ obtained from FHT requires s time steps for a first-order RM code located at the s -th stage [37]. Furthermore, for the sequential implementation, the permutation selection in (3) requires s time steps if $r_\lambda \geq 2$ and s^2 time steps if $r_\lambda = 1$, since each permutation is evaluated sequentially. In the parallel implementation of (3), a single time step is required if $r_\lambda \geq 2$ and s time steps are required if $r_\lambda = 1$. In addition, the hard decisions obtained from the LLR values and binary operations are computed instantaneously [17], [21], [22]. Finally, we assume that the number of time steps required by a merge sort algorithm to sort an array of N elements is $\log_2(N)$ [38, Chapter 2]. We also use similar assumptions to compute the decoding latency of all the other decoders considered in this paper.

To calculate the computational complexity of the decoders considered in this paper, we count the number of floating point operations, namely, the number of additions, subtractions, and comparisons, required during the course of decoding. Note that the merge sort algorithm requires $N \log_2 N$ comparisons to sort an array of length N [38, Chapter 2].

2) *Comparison with FSCL, SC-Stack and SP-SCL Decoding Algorithms:* Fig. 6 provides the error-correction performance in terms of FER of the proposed decoders and that of the FSCL, SC-Stack (SCS), and SP-SCL decoders for $\mathcal{RM}(r, 9)$, $r \in \{2, 3, 4\}$. The SCS decoder considered

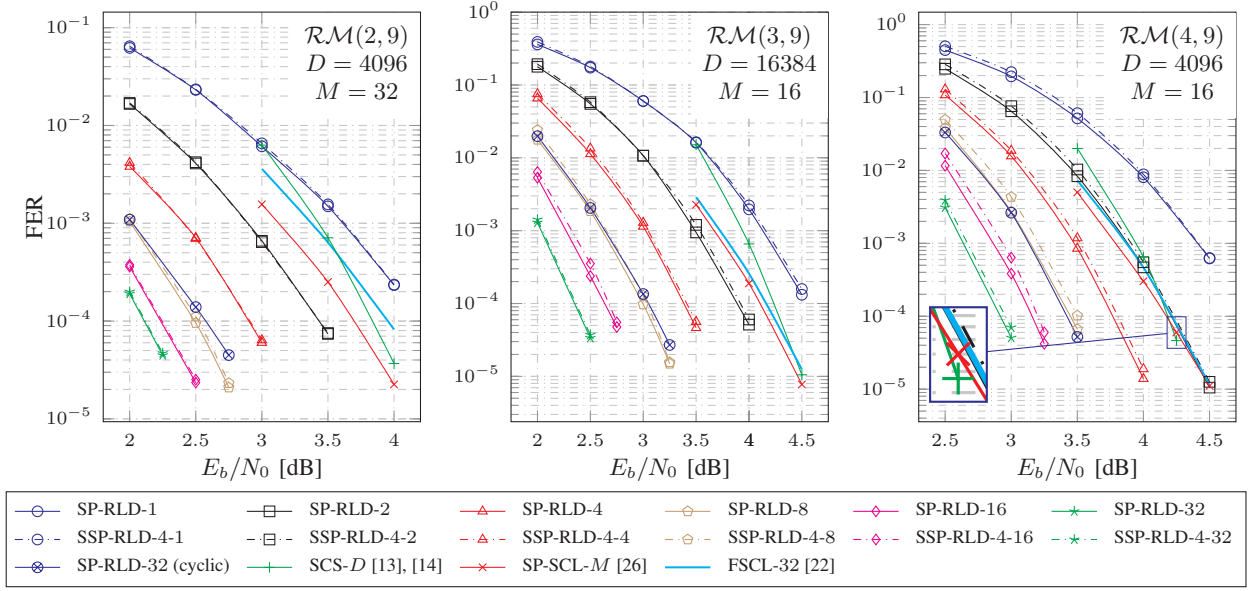


Fig. 6: Error-correction performance of the proposed decoders and that of the SCS, SP-SCL, and FSCL decoders.

in this paper utilizes the enhanced score function introduced in [14] to reduce the stack size when compared with the conventional SCS decoder introduced in [13]. In Fig. 6, the SCS decoder with stack size D is denoted as SCS- D , while the SP-SCL decoder with list size M is denoted as SP-SCL- M . The values of D and M are selected to allow an FER performance comparable to that of the FSCL decoder with list size 32 (FSCL-32). With $S = 4$, the SSP-RLD decoder has a negligible error-correction performance degradation when compared to the SP-RLD decoder with the same list size. Furthermore, we also provide the FER performance of the proposed SP-RLD-32 decoder where only cyclic factor-graph permutations are considered.

It can be observed from Fig. 6 that the FER of the SP-RLD-32 decoder with cyclic factor-graph permutations is relatively similar to that of the SP-RLD-8 decoder with the codeword permutations sampled from the full symmetry group. In addition, at no additional cost, the SP-RLD-32 decoder that utilizes the general codeword permutations obtains a maximum gain of 0.7 dB at the target FER of 10^{-4} , when compared to the SP-RLD-32 decoder that only uses cyclic factor-graph permutations.

Fig. 7 illustrates the computational complexity (\mathcal{C}) and decoding latency (\mathcal{T}) of SP-RLD- L and SSP-RLD-4- L under the sequential and parallel implementations of the proposed SP scheme. In addition, the memory requirement (\mathcal{M}) in kilobytes (KBs) of SP-RLD- L and SSP-RLD-4- L

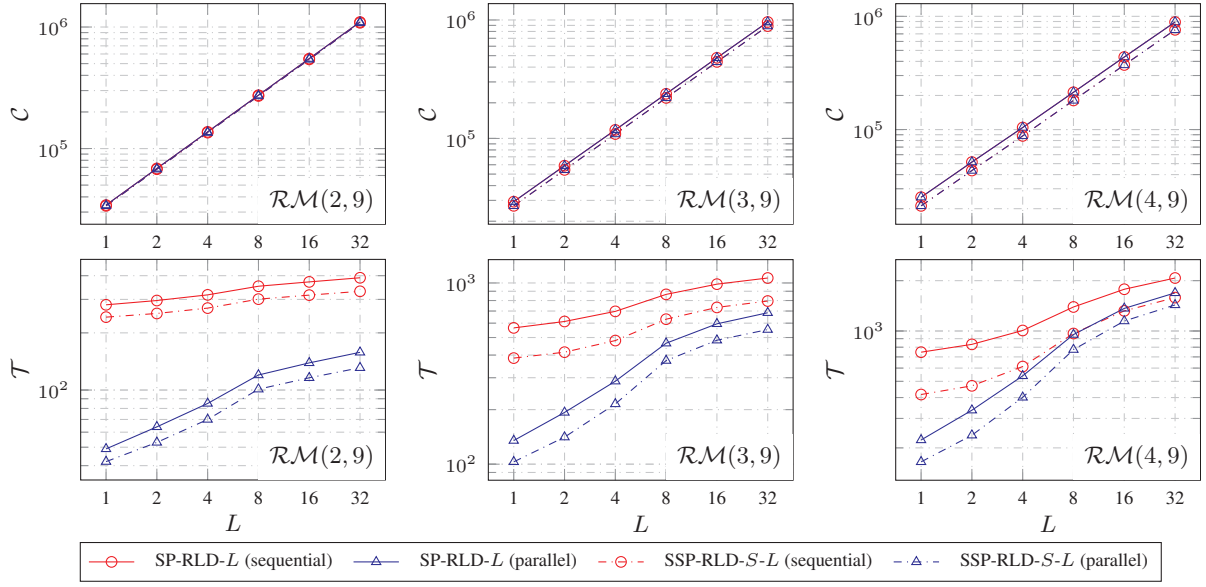


Fig. 7: Computational complexity and decoding latency of the proposed decoders under the sequential and parallel implementations of the SP scheme.

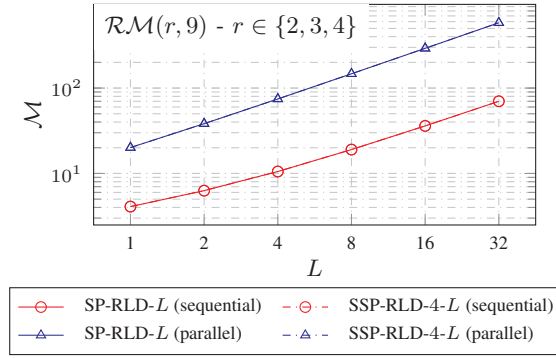


Fig. 8: Memory consumption in KBs of the proposed decoders whose FER curves are provided in Fig 6.

is provided in Fig. 8. It can be observed from Fig. 7 that the SSP-RLD-4- L decoder relatively maintains the computational complexity when compared with SP-RLD- L . However, SSP-RLD-4- L significantly reduces the decoding latency of SP-RLD- L while only incurring negligible error-correction performance degradation as seen from Fig 6. Furthermore, Fig. 7 and Fig. 8 reveal the trade-offs between the decoding latency and memory requirement of the proposed decoders under the sequential and parallel implementations of the SP scheme. In particular, the improvements in the decoding latency of the parallel implementation over the sequential implementation come at the cost of memory consumption overheads.

TABLE II: Comparison of computational complexity (\mathcal{C}), decoding latency in time steps (\mathcal{T}), and memory requirement in KBs (\mathcal{M}) of SCS, SP-SCL, FSCL, and proposed SSP-RLD decoders considered in Fig 6.

	SCS- D [13], [14]				SP-SCL- M [26]				FSCL-32 [22]			SSP-RLD-4-2				
	D	\mathcal{C}	\mathcal{T}	\mathcal{M}	M	\mathcal{C}	\mathcal{T}	\mathcal{M}	\mathcal{C}	\mathcal{T}	\mathcal{M}	\mathcal{C}	\mathcal{T}_s	\mathcal{M}_s	\mathcal{T}_p	\mathcal{M}_p
$\mathcal{RM}(2, 9)$	4096	4.17E+7	3.04E+5	8208	32	8.45E+5	1.85E+3	70	9.59E+4	373	70	6.75E+4	253	6.3	53	38.3
$\mathcal{RM}(3, 9)$	16384	4.79E+6	9.94E+3	32832	16	4.34E+5	2.30E+3	36	1.55E+5	1039	70	5.43E+4	415	6.3	141	38.3
$\mathcal{RM}(4, 9)$	8192	1.06E+7	4.15E+4	16416	16	4.55E+5	3.06E+3	36	2.24E+5	1991	70	4.34E+4	470	6.3	238	38.3

Table II summarizes the memory requirement in KBs, the computational complexity, and the decoding latency in time steps of FSCL, SCS, and SP-SCL decoders, and those of the SSP-RLD decoder with $L = 2$ and $S = 4$, whose FER values are plotted in Fig 6. Note that for the SSP-RLD-4-2 decoder, \mathcal{T}_s and \mathcal{M}_s indicate the decoding latency and memory requirement of the sequential implementation, while \mathcal{T}_p and \mathcal{M}_p indicate the decoding latency and memory requirement of the parallel implementation of the SP scheme, respectively. It can be seen in Fig. 6 that the FER performance of SSP-RLD-4-2 is similar to or better than that of the FSCL, SCS and SP-SCL decoders at the target FER of 10^{-4} for all the considered RM codes. In addition, under both sequential and parallel implementations of the SP scheme, SSP-RLD-4-2 significantly outperforms FSCL, SCS, and SP-SCL decoders in various complexity metrics as shown in Table II.

3) *Comparison with State-of-the-Art RM Decoders:* Fig. 9 compares the FER performance of the proposed SSP-RLD decoder with that of the state-of-the-art decoders for various RM codes. We consider the RLDP [20] and the RLDA [20], [28] algorithms with list size M , the simplified SC (SSC) decoder [36] when applied to P factor-graph permutations (Per-SSC- P) [27], and P general permutations (Aut-SSC- P) sampled from the full symmetry group of the codes [28]. The error-correction performance of the ML decoder [20] and that of the sparse-RPA (SRPA) decoder introduced in [24] are also plotted in Fig. 9. Table III summarizes the computational complexity, decoding latency, and memory requirement of SRPA, Aut-SSC- P , RLDA- M , and the proposed SSP-RLD- S - L decoders in Fig 9, which have a comparable error-correction performance at the target FER of 10^{-3} for all the considered RM codes. Note that a fully-parallel implementation of the SRPA decoder, in which all the operations that can be carried out concurrently are executed at the same time, is considered. The SRPA decoding algorithm runs two fully-parallel RPA decoders with each decoder using a quarter of the code projections

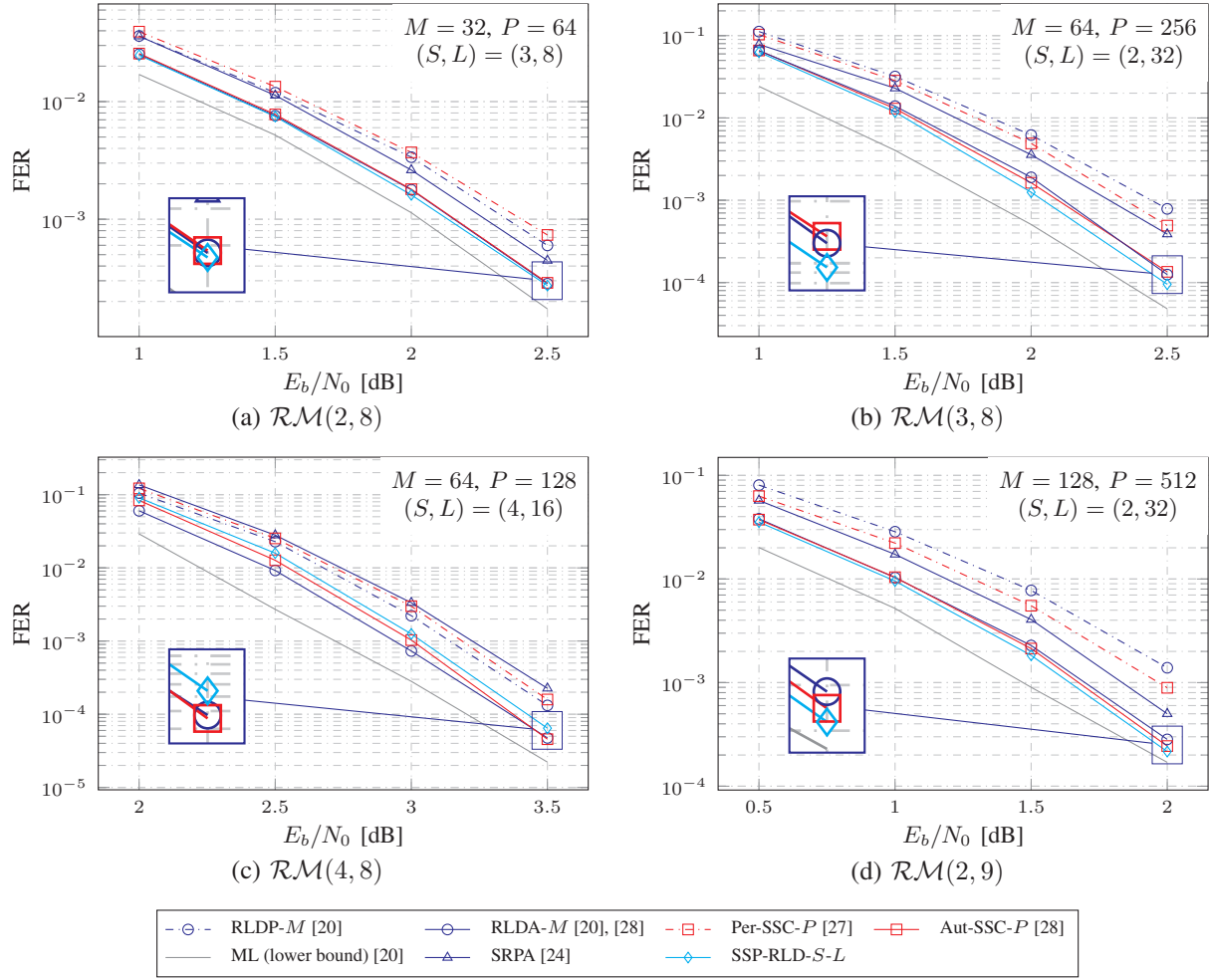


Fig. 9: Error-correction performance of various permutation decoding algorithms of RM codes. The FER of the SRPA decoder and the ML lower-bound are also plotted for comparison.

at each recursion step [24]. Thus, the SRPA decoder effectively reduces 50% of the total number of projections used by the conventional RPA algorithm [23]. This configuration incurs negligible error-correction performance loss with respect to the conventional RPA decoder in [23] for the second and third order RM codes of size 256.

It can be seen in Fig. 9 that with the same list size M or the same number of permutations P , using the permutations randomly sampled from the full symmetry group of the codes provides significant error-correction performance improvement for RLDA- M and Aut-SSC- P decoders at no additional cost, compared to the RLDP- M and Per-SSC- P decoders, respectively. In addition, as observed from Fig. 9 and Table III, all permutation decoding algorithms, RLDA, Aut-SSC, and SSP-RLD, provide significantly better error-correction performance compared to the SRPA

TABLE III: Comparison of computational complexity (\mathcal{C}), decoding latency in time steps (\mathcal{T}), and memory requirement in KBs (\mathcal{M}) of various RM decoders considered in Fig. 9.

	SRPA [24]			Aut-SSC- P [28]				RLDA- M [20], [28]				SSP-RLD- $S-L$							
	\mathcal{C}	\mathcal{T}	\mathcal{M}	P	\mathcal{C}	\mathcal{T}	\mathcal{M}	M	\mathcal{C}	\mathcal{T}	\mathcal{M}	S	L	\mathcal{C}	\mathcal{T}_s	\mathcal{M}_s	\mathcal{T}_p	\mathcal{M}_p	
$\mathcal{RM}(2, 8)$	6.5E+5	3592	69.2	64	9.4E+4	80	129.8	32	5.2E+4	299	35	3	8	1.0E+5	195	9.5	67	65.5	
$\mathcal{RM}(3, 8)$	7.9E+7	6184	281.5	256	4.5E+5	292	259.5	64	1.8E+5	825	69.0	2	32	2.4E+5	426	35.0	358	259.0	
$\mathcal{RM}(4, 8)$	3.6E+9	7816	465.2	128	2.2E+5	165	259.5	64	2.6E+5	1409	69.0	4	16	1.6E+5	903	18.0	721	130.0	
$\mathcal{RM}(2, 9)$	3.4E+6	10250	271.61	512	1.5E+6	106	2078.0	128	4.1E+5	452	274	2	32	9.5E+5	228	70.0	100	582.0	

decoder with significantly lower computational complexity and decoding latency for various RM code configurations.

When the sequential implementation is considered, the proposed SSP-RLD decoder is the most memory efficient decoding algorithm among all the permutation decoders, while the Aut-SSC decoder has the smallest decoding latency. For $\mathcal{RM}(3, 8)$, the sequential implementation of the proposed decoder reduces 48% of the decoding latency and 49% of the memory consumption compared to RLDA-64 with a similar FER performance, while introducing a 32% computational complexity overhead. On the other hand, compared to Aut-SSC-256 for $\mathcal{RM}(3, 8)$ at a similar FER performance, the sequential SSP-RLD-2-32 decoder reduces 47% of the computational complexity and 86% of the memory consumption, at the cost of $1.45\times$ increase in the decoding latency. For $\mathcal{RM}(4, 8)$, the sequential SSP-RLD-4-16 decoder reduces 39% of the computational complexity, 36% of the decoding latency, and 74% of the memory requirement, while only incurring an error-correction performance degradation of 0.1 dB at the target FER of 10^{-3} , compared to RLDA-64. For the same RM code and at the target FER of 10^{-3} , SSP-RLD-4-16 reduces 27% of the computational complexity and provides a memory reduction of $14.4\times$ compared to Aut-SSC-128. These improvements come at the cost of $5.5\times$ increase in the decoding latency and a negligible FER performance degradation compared to Aut-SSC-128.

Under the parallel implementation of the proposed decoder for $\mathcal{RM}(2, 8)$ and $\mathcal{RM}(3, 9)$, SSP-RLD can provide competitive performance trade-offs in comparison with Aut-SSC decoder. In particular, for the case of $\mathcal{RM}(2, 8)$, the decoding latency and memory requirement of the parallel SSP-RLD-3-8 are only 84% and 50% of those of Aut-SSC-64, respectively, while only incurring 6% of computational overhead at a similar error-correction performance. Furthermore, at a similar FER and decoding latency for the case of $\mathcal{RM}(2, 9)$, the parallel SSP-RLD-2-32 reduces 37% of the computational complexity and 72% of the memory consumption compared

to Aut-SSC-512.

IV. CONCLUSION

In this paper, a novel successive permutation (SP) scheme is proposed to significantly improve the error-correction performance of Reed-Muller (RM) codes under an improved recursive list decoding (RLD) algorithm. In particular, we performed low-complexity maximum likelihood (ML) decoding on the rich symmetry group of RM codes to select a good permutation of the code on the fly. An efficient decoding latency reduction scheme was introduced that incurs a negligible error-correction performance degradation. We performed a numerical analysis of the proposed decoder in terms of error-correction performance, computational complexity, decoding latency, and memory requirement and compares them with those of the state-of-the-art RM decoders. The simulation results confirmed the effectiveness of the proposed decoder under various configurations of RM codes. Specifically, for the RM codes of sizes 256 and 512 with order 2, the parallel implementation of the proposed decoder results in a slightly better decoding latency when compared to the simplified successive cancellation decoder with random codeword permutations, while reducing 50% and 72% of the memory requirement, respectively, at the target frame error rate of 10^{-3} .

REFERENCES

- [1] D. E. Muller, "Application of boolean algebra to switching circuit design and to error detection," *Transactions of the I.R.E. Professional Group on Electronic Computers*, vol. EC-3, no. 3, pp. 6–12, 1954.
- [2] I. Reed, "A class of multiple-error-correcting codes and the decoding scheme," *Transactions of the IRE Professional Group on Information Theory*, vol. 4, no. 4, pp. 38–49, 1954.
- [3] S. Kudekar, S. Kumar, M. Mondelli, H. D. Pfister, E. Şaşoğlu, and R. L. Urbanke, "Reed-muller codes achieve capacity on erasure channels," *IEEE Trans. Inf. Theory*, vol. 63, no. 7, pp. 4298–4316, 2017.
- [4] R. Pedarsani, S. H. Hassani, I. Tal, and E. Telatar, "On the construction of polar codes," in *IEEE Int. Symp. on Inf. Theory*, 2011, pp. 11–15.
- [5] P. Trifonov, "Efficient design and decoding of polar codes," *IEEE Trans. Commun.*, vol. 60, no. 11, pp. 3221–3227, 2012.
- [6] I. Tal and A. Vardy, "How to construct polar codes," *IEEE Trans. Inf. Theory*, vol. 59, no. 10, pp. 6562–6582, 2013.
- [7] M. Mondelli, S. H. Hassani, and R. Urbanke, "Construction of polar codes with sublinear complexity," in *IEEE Int. Symp. on Inf. Theory*, 2017, pp. 1853–1857.
- [8] L. Huang, H. Zhang, R. Li, Y. Ge, and J. Wang, "Reinforcement learning for nested polar code construction," *IEEE Global Commun. Conf.*, pp. 1–6, 2019.
- [9] Y. Liao, S. A. Hashemi, J. M. Cioffi, and A. Goldsmith, "Construction of polar codes with reinforcement learning," *IEEE Trans. Commun.*, vol. 70, no. 1, pp. 185–198, 2022.

- [10] E. Arkan, "Channel polarization: A method for constructing capacity-achieving codes for symmetric binary-input memoryless channels," *IEEE Trans. Inf. Theory*, vol. 55, no. 7, pp. 3051–3073, July 2009.
- [11] N. Hussami, S. B. Korada, and R. Urbanke, "Performance of polar codes for channel and source coding," in *IEEE Int. Symp. on Inf. Theory*, 2009, pp. 1488–1492.
- [12] G. Schnabl and M. Bossert, "Soft-decision decoding of Reed-Muller codes as generalized multiple concatenated codes," *IEEE Transactions on Information Theory*, vol. 41, no. 1, pp. 304–308, 1995.
- [13] K. Niu and K. Chen, "Stack decoding of polar codes," *Electronics letters*, vol. 48, no. 12, pp. 695–697, 2012.
- [14] P. Trifonov, "A score function for sequential decoding of polar codes," in *2018 IEEE International Symposium on Information Theory (ISIT)*, 2018, pp. 1470–1474.
- [15] I. Tal and A. Vardy, "List decoding of polar codes," *IEEE Trans. Inf. Theory*, vol. 61, no. 5, pp. 2213–2226, March 2015.
- [16] K. Niu and K. Chen, "CRC-aided decoding of polar codes," *IEEE Communications Letters*, vol. 16, no. 10, pp. 1668–1671, 2012.
- [17] A. Balatsoukas-Stimming, M. B. Parizi, and A. Burg, "LLR-based successive cancellation list decoding of polar codes," *IEEE Trans. Signal Process.*, vol. 63, no. 19, pp. 5165–5179, Oct. 2015.
- [18] I. Dumer, "Recursive decoding and its performance for low-rate Reed-Muller codes," vol. 50, no. 5. IEEE, 2004, pp. 811–823.
- [19] I. Dumer and K. Shabunov, "Recursive list decoding for reed-muller codes and their subcodes," pp. 279–298, 2002. [Online]. Available: https://doi.org/10.1007/978-1-4757-3585-7_17
- [20] I. Dumer and K. Shabunov, "Soft-decision decoding of Reed-Muller codes: recursive lists," *IEEE Trans. Inf. Theory*, vol. 52, no. 3, pp. 1260–1266, 2006.
- [21] M. H. Ardakani, M. Hanif, M. Ardakani, and C. Tellambura, "Fast successive-cancellation-based decoders of polar codes," *IEEE Trans. Commun.*, vol. 67, no. 7, pp. 4562–4574, 2019.
- [22] S. A. Hashemi, C. Condo, and W. J. Gross, "Fast and flexible successive-cancellation list decoders for polar codes," *IEEE Trans. on Sig. Proc.*, vol. 65, no. 21, pp. 5756–5769, Nov 2017.
- [23] M. Ye and E. Abbe, "Recursive projection-aggregation decoding of Reed-Muller codes," *IEEE Trans. Inf. Theory*, vol. 66, no. 8, pp. 4948–4965, 2020.
- [24] D. Fathollahi, N. Farsad, S. A. Hashemi, and M. Mondelli, "Sparse multi-decoder recursive projection aggregation for Reed-Muller codes," in *2021 IEEE International Symposium on Information Theory (ISIT)*, 2021, pp. 1082–1087.
- [25] J. D. Key, T. P. McDonough, and V. C. Mavron, "Reed-Muller codes and permutation decoding," *Discrete mathematics*, vol. 310, no. 22, pp. 3114–3119, 2010.
- [26] S. A. Hashemi, N. Doan, M. Mondelli, and W. J. Gross, "Decoding Reed-Muller and polar codes by successive factor graph permutations," in *2018 IEEE 10th International Symposium on Turbo Codes Iterative Information Processing (ISTC)*, 2018, pp. 1–5.
- [27] M. Kamenev, Y. Kameneva, O. Kurmaev, and A. Maevskiy, "A new permutation decoding method for Reed-Muller codes," in *IEEE Int. Symp. on Inf. Theory*, 2019, pp. 26–30.
- [28] M. Geiselhart, A. Elkelesh, M. Ebada, S. Cammerer, and S. t. Brink, "Automorphism ensemble decoding of reed-muller codes," *IEEE Trans. Commun.*, vol. 69, no. 10, pp. 6424–6438, 2021.
- [29] S. B. Korada, "Polar codes for channel and source coding," Ph.D. dissertation, EPFL, Lausanne, Switzerland, 2009.
- [30] A. Elkelesh, M. Ebada, S. Cammerer, and S. ten Brink, "Belief propagation list decoding of polar codes," *IEEE Commun. Letters*, vol. 22, no. 8, pp. 1536–1539, 2018.
- [31] N. Doan, S. A. Hashemi, M. Mondelli, and W. J. Gross, "On the decoding of polar codes on permuted factor graphs," *IEEE Global Commun. Conf.*, pp. 1–6, Dec 2018.

- [32] N. Doan, S. A. Hashemi, and W. J. Gross, "Decoding polar codes with reinforcement learning," *IEEE Global Commun. Conf.*, pp. 1–6, 2020.
- [33] M. Geiselhart, A. Elkelesh, M. Ebada, S. Cammerer, and S. ten Brink, "CRC-aided belief propagation list decoding of polar codes," in *2020 IEEE International Symposium on Information Theory (ISIT)*, 2020, pp. 395–400.
- [34] E. Arikan, "A survey of Reed-Muller codes from polar coding perspective," in *IEEE Inf. Theory Work. on Inf. Theory*, 2010, pp. 1–5.
- [35] F. J. MacWilliams and N. J. A. Sloane, *The theory of error-correcting codes*. Elsevier, 1977.
- [36] G. Sarkis, P. Giard, A. Vardy, C. Thibault, and W. J. Gross, "Fast polar decoders: Algorithm and implementation," *IEEE J. Sel. Areas Commun.*, vol. 32, no. 5, pp. 946–957, April 2014.
- [37] Y. Be'ery and J. Snyders, "Optimal soft decision block decoders based on fast Hadamard transform," *IEEE Trans. Inf. Theory*, vol. 32, no. 3, pp. 355–364, 1986.
- [38] T. H. Cormen, C. E. Leiserson, R. L. Rivest, and C. Stein, *Introduction to algorithms*. MIT press, 2009.